Engineering Conferences International
ECI Digital Archives

The 14th International Conference on Fluidization – From Fundamentals to Products

Refereed Proceedings

2013

Gas Backmixing Study in a CFB Downer Gassolids Separator

Martin R.J. Huard
(ICFAR), Western University, Canada

Franco Berruti
(ICFAR), Western University, Canada

Cedric L. Briens
(ICFAR), Western University, Canada

GAS BACKMIXING STUDY IN A CFB DOWNER GAS-SOLIDS SEPARATOR

Martin R.J. Huard[a]*, Franco Berruti[a] and Cedric L. Briens[a]
[a] Institute for Chemicals and Fuels from Alternative Resources (ICFAR), Western University;
22312 Wonderland Road North, N0M 2A0, Ilderton, Ontario, Canada
*T: 1-519-661-3885; F: 1-519-661-4016; E: mhuard3@uwo.ca

ABSTRACT
A simple pressure measurement technique was developed to measure the extent of gas backmixing in the gas-solids separator of a circulating fluidized bed downer reactor. Several separator designs were screened according to their particle collection efficiency and backmixing. A 60° cone-shaped particle deflector with a 6.3 cm diameter rim was selected as the best separator design.

INTRODUCTION
Previous residence time distribution (RTD) studies in circulating fluidized bed (CFB) reactors have often neglected the impact of the reactor outlet and gas-solids separator on backmixing (gas or solids) in the unit. However, Harris et al. (1) showed that the geometry of a riser exit can have a significant effect on the reactor hydrodynamics. When compared to the more traditional CFB risers, CFB downers benefit from a nearly plug flow behavior of both gas and particles, and are attractive for processes such as heavy oil or biomass pyrolysis, where backmixing would result in the overcracking of valuable products. It is, therefore, essential that the gas-solids separator, at the downer exit, does not introduce major backmixing of gas or particles.

The purpose of this study is, therefore, to take downer separator geometries identified in preliminary studies from Huard et al. (2-3), measure their impact on backmixing in a cold model and adjust their geometry to minimize backmixing while maintaining efficient gas-solids separation. The cold model used in this study represented a same scale pilot plant downer used for heavy oil or biomass pyrolysis.

BACKGROUND
Previous RTD studies in CFB downer units have typically used a form of the axial dispersion model, e.g. Brust and Wirth (4), to describe the RTD in the downer. However, the impact of the gas-solids separator on the overall downer RTD has not been investigated. The two-parameter axial dispersion model does not provide a good fit of tracer pulse response data measured in the gas-solids separator. This study uses, instead, combinations of two-parameter, asymmetrical peak exponential distributions $G_i(t)$, where t is the time:

$$G_i(t) = 4a_i \exp\left[\frac{-2(t-t_{0i})}{a_i}\right]\left\{1-\exp\left[\frac{-2(t-t_{0i})}{a_i}\right]\right\} \quad (1)$$

where a_i is the peak amplitude and t_{0i} is the initial peak time, i.e. the time at which the signal starts increasing above its baseline of 0. Note that this assumes that the area enclosed by $G_i(t)$, A_{Gi}, is unity, as for a true RTD (5).

Pulse response curves can be fitted with increasing accuracy by summing several weighted expressions $G_i(t)$ of the form given in Equation (1):

$$G(t) = \sum_{i=1}^{N} \alpha_i G_i(t), \quad (2)$$

where α_i is the weight factor for the peak function $G_i(t)$. To preserve the condition $A_G = 1$, all α_i must sum to unity, since $A_{Gi} = 1$ for all $G_i(t)$. The weight factor α_N for the last term $G_N(t)$ in Equation (2) can be written in terms of the other weight factors:

$$\alpha_N = 1 - \sum_{i=1}^{N-1} \alpha_i \, . \quad (3)$$

Finally, for use in downstep response experiments, it can be shown that the normalized discrete cumulative distribution $H(t_j)$ at time t_j is related to the discrete peak distribution $G(t_j)$ by:

$$H(t_j) = H(t_{j-1}) - G(t_j) \Big/ \sum_{j=1}^{\infty} G(t_j) \, ; \; 0 \le j \le \infty, \; H(t_0) = 1. \quad (4)$$

Each experimental downstep response curve $Y(t)$ was fitted by minimizing the residual error between the fitting function $H(t)$ and $Y(t)$ by adjusting the parameters in Equations (1) and (2) using an iterative solver.

MATERIALS & METHOD

A cold model downer similar to the one used in (2-3) was used to perform gas phase step response measurements. The downer had an internal diameter (D) of 7.0 cm and a total height (H) of 134 cm, as indicated in Fig. 1(a). Several gas-solids separator designs were tested, including: three sizes of a 60° internal angle cone-shaped particle deflector, and a bell-shaped deflector. The geometry for each shape tested is shown in Figs. 1(e) to 1(i). The vertical position of each separator shape was fixed such that the bottom edge of any given shape was at the same height as the gas outlet. Compressed air at room temperature was used as the carrier gas in the downer. The range of superficial gas velocities in the downer was 0.80 m/s ≤ U_g ≤ 1.30 m/s. Silica sand with a Sauter mean diameter of 200 μm was used for the solids phase. The range of solids loading F_s/F_g in the downer was 0 to 15 kg/kg. Solids were fed to the downer inlet by a calibrated gravity flow system. Gas and solids were mixed in a Y-shaped pipe fitting at the downer inlet.

During each downstep experiment, helium tracer was injected steadily then cut off sharply in a downstep into the bulk air flow in the downer by a solenoid valve. Tracer was detected by measuring the corresponding change in the pressure drop of the bulk flow across the gas-solids separator, i.e. between locations P_1 and P_2 as shown in Fig. 1(b) due to the change in gas composition. The pressure drop between P_1 and P_2 was measured using a calibrated, fast-response, differential pressure transducer with a range of 34 kPa. A 5 cm diameter circular ring sparger with 18 horizontal-pointing 0.08 cm diameter holes spaced equally around the ring was used to distribute tracer over the downer cross section. The sparger was located 14 cm, i.e. two downer diameters, above the gas outlet. The steady state concentration of helium during tracer injection was 5 vol.%, which was assumed not to have a significant effect on the downer hydrodynamics. To verify this assumption, the pulse responses for steady state helium

concentrations of 3 vol.%, 5 vol.%, and 7 vol.% were compared using the smallest 60° cone and gas velocity U_g = 0.80 m/s. The standard deviation of the pulse responses varied less than 10% between runs, which was deemed adequate. The gage pressure was also measured at location P_3, as shown in Fig. 1(b). All pressure data were sampled at 500 Hz by a data acquisition system.

To prevent significant dispersion and backmixing of tracer across the detection boundary at P_1, two rows of criss-cross pattern sheds were mounted in the downer just upstream of the gas-solids separator. Each row consisted of three sheds and occupied one half of the downer cross section, as shown in Figs. 1(b) and 1(c). The sheds prevented backmixing. In this way the sheds created an approximation to a true closed boundary condition essential to accurate RTD measurement (6). The sparger ring for the tracer distribution, described above, was mounted to the bottom surface of the sheds.

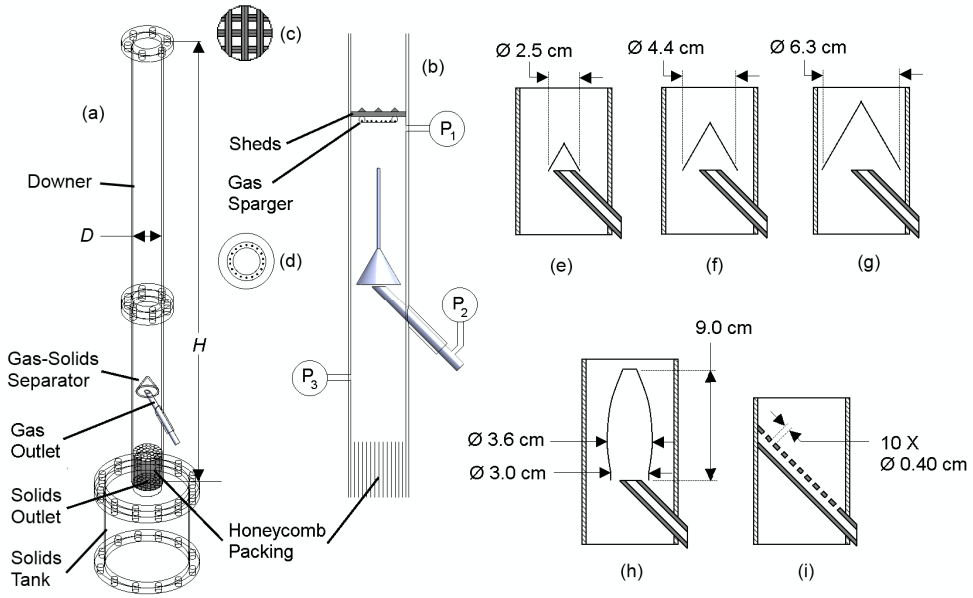

Figure 1 – Illustration of Experimental Apparatus: (a) Apparatus Isometric View; (b) Gas-Solids Separation Zone Elevation View; (c) Sheds Plan View; (d) Gas Sparger Injector Plan View; (e) "Small" 60° Cone; (f) "Medium" 60° Cone; (g) "Large" 60° Cone

RESULTS & DISCUSSION

Separator Pressure Drop Measurement Technique

Huard et al. (2) demonstrated a hot wire anemometer measurement technique to detect helium tracer in a gas-only downer. This hot wire method could not be adapted successfully for a multiphase system with solids. Despite measures taken to minimize the effect of gas sampling lines used to protect the hot wires, significant gas backmixing occurred in the sampling lines which prevented accurate measurement of the downer and separator step response. Therefore, a simple, robust pressure measurement technique was developed to measure the separator response to a helium tracer downstep.

The response in the pressure drop across the gas-solids separator to a helium tracer downstep was used to detect the tracer. A sample pressure drop signal

during a downstep experiment is shown in Fig. 2, which demonstrated good sensitivity to a helium tracer concentration of 5 vol.% in air. The pressure drop was then used to determine the instantaneous transient helium concentration of the gas exiting though the separator gas outlet tube during a downstep experiment. This method uses the fact that most of the pressure drop in the separator section is concentrated at the separator gas exit. A calibration curve of helium concentration versus separator pressure drop transducer voltage was generated for each separator design and superficial gas velocity (U_g). Small, steady state helium injections between 0 and 7 vol.% were used to produce the calibration curves, of which a sample is shown in Fig. 3. All calibration curves were fitted well with simple quadratic polynomial expressions. Finally, in turn, the helium concentration response curve from each experiment was normalized and used to obtain the cumulative step response function $H(t)$.

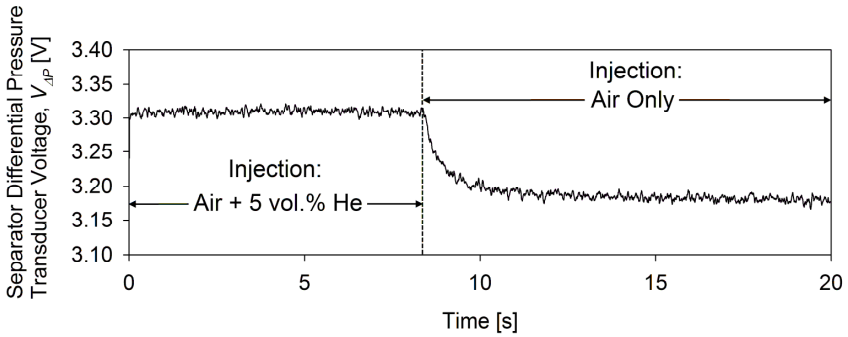

Figure 2 – Sample Separator Pressure Drop Signal

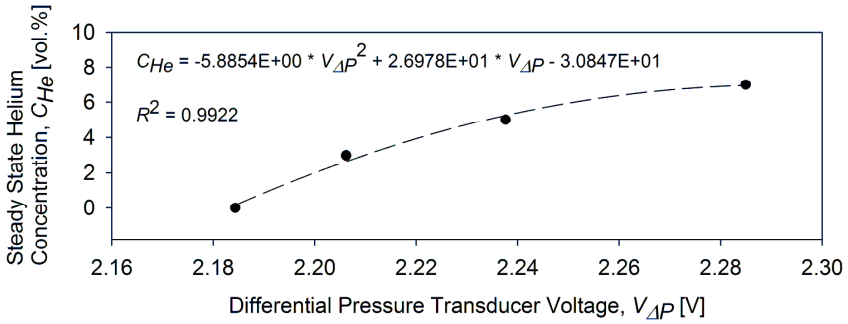

Figure 3 – Sample Calibration Curve for Helium Concentration versus Pressure Transducer Voltage (U_g = 0.80 m/s, 60° large cone design, no solids)

Gas Recirculation in Solids Collection Tank

Preliminary tests showed that the separator pressure drop increased significantly with the solids collection tank fill level when a honeycomb packing was not used in the solids outlet. This effect had a substantial negative impact on gas backmixing and the standard deviation of the separator pulse response. When the solids tank was empty, gas penetrated to and recirculated in the large solids tank, whose volume was much larger than the reactor. An empty tank allowed significant gas backmixing, which was indicated by large standard deviation values in the pulse response. However, when the tank was full with solids, the overall unit volume decreased and prevented gas from recirculating in the tank, thereby eliminating a source of backmixing. As shown in Fig. 4, the standard deviation σ in the separator pulse response increased with the gas velocity with an empty tank. However, with a full tank, backmixing was greatly reduced at gas

velocities of 1.05 m/s and 1.30 m/s. A honeycomb packing was, therefore, installed at the solids outlet to induce a large pressure drop across the outlet, thereby reducing gas backmixing in the solids tank (Fig. 1). It simulates the restriction to gas flow that would result from the presence of a stripper at the same location in an industrial downer unit (the stripper would be used to recover product vapors).

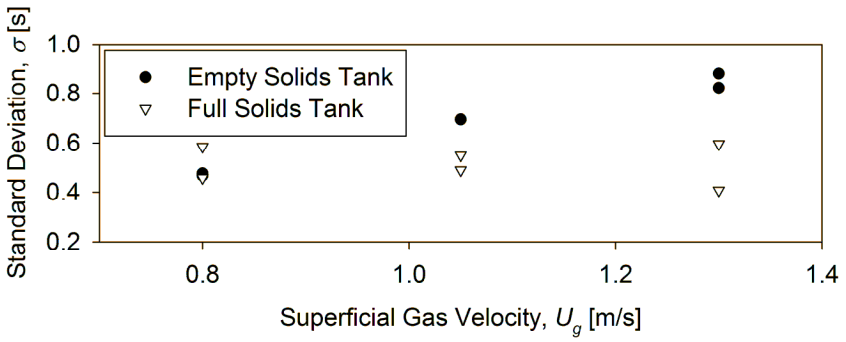

Figure 4 - Effect of Solids Tank Fill Level and Superficial Gas Velocity on Gas Backmixing (without solids)

Minimal Backmixing Baseline Case

A baseline case was established to account for the gas backmixing induced by the sheds, tracer sparger injector, and the gas and solids outlet during all experiments. The baseline case was also devised to characterize a state of minimal backmixing with an ideal, if impractical, separator that would minimize gas backmixing. In this case, a special gas outlet pipe with sparger holes spanning the downer diameter was used as a gas outlet for the entire downer. This special gas outlet had ten, 4 mm diameter sparger holes as shown in Fig. 1(i). The gas outlet was mounted at an angle of 45° relative to the downer's vertical axis, using the same mounting port as the normal gas outlet pipe used in all other experiments. The pulse response for the baseline case is represented by a heavy black plot in Fig. 6. With this ideal separator, a relatively sharp response to a tracer downstep was measured without solids present, indicating minimal gas backmixing. In this case, gas was minimally obstructed from exiting the downer via the gas outlet pipe.

Impact of Separator Design on Separator Gas Backmixing

Figure 5 shows that the method described in the Background section can provide a very good fit of the experimental response curves. The fitted curves were used to calculate the response to a Dirac pulse tracer injection, as well as the sum of the squared residual between the pulse response for a given separator design and the ideal separator.

The backmixing induced by each of the separator designs was compared to the baseline case. When any one of the separator designs was mounted in the separation zone, the separator pulse response without solids was smeared and reached steady state at a longer time relative to the baseline case, as shown in Fig. 6, indicating significant backmixing. The pulse response for each separator design is compared to the baseline case in Fig. 6 for a superficial gas velocity U_g = 0.80 m/s and without solids. By simple visual comparison of the pulse response

plots, any given separator design could be screened quickly for its impact on backmixing using the pressure drop measurement technique.

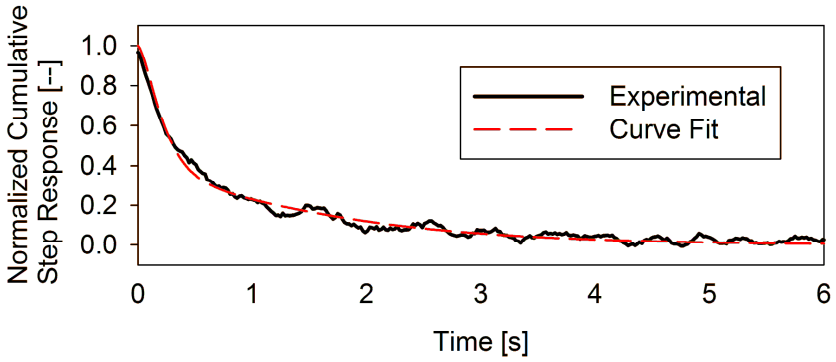

Figure 5 – Sample Fit of Downstep Response Data (bell-shaped design, U_g = 0.80 m/s, no solids)

Among the cone-shaped separator designs, the extent of backmixing increased as the cone size decreased. Increased backmixing was indicated by pulse responses with multiple peaks and longer tails, as shown in Fig. 6. Overall, the least extensive backmixing was observed for the largest cone size. Meanwhile, the pulse response of the bell-shaped separator design was similar to the medium sized 60° cone. Among the cone shaped separators, as the cone size decreased, the exit gap size between the gas outlet and the cone rim also decreased. Decreasing cone size caused the gas to accelerate to higher velocity through the exit gap, which was surmised to give greater fluid exchange with gas flowing downward near the downer wall, leading to more backmixing. A simple mass transfer calculation was performed to determine the exchange between these two counter-current gas streams and was found to be highest in the smallest cone size. Furthermore, the mass transfer between the two streams decreased with increasing cone size. Hence, the results in Fig. 6 are in agreement with the mass transfer calculation and demonstrate that most of the gas backmixing in the separator occurs near the gas outlet, where the local gas velocity is greatest.

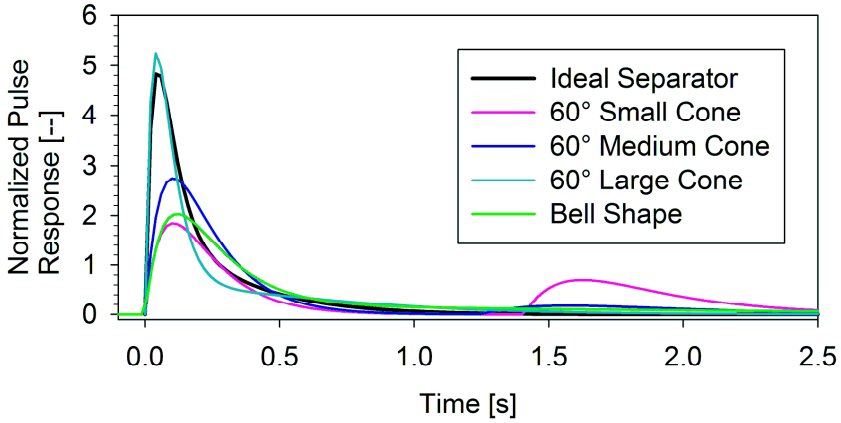

Figure 6 - Comparison of Pulse Responses for Various Separator Designs (U_g = 0.80 m/s; no solids)

Effect of Solids Loading on Separator Gas Backmixing

For each separator design, the residual difference between the pulse responses for an ideal separator and a given separator design was calculated. Larger residuals between the pulse responses indicated extensive gas backmixing relative to the baseline case. Shown in Fig. 7 are plots of the sum of the squared residual, *S*, as a function of the solids loading for all tested separator designs. In general, the deviation from an ideal separator increased with the solids loading for all separator shapes except for the medium-sized 60° cone. At all solids loadings, the largest 60° cone showed the smallest difference from an ideal separator. Hence, the least extensive backmixing relative to an ideal separator was observed using the large 60° cone.

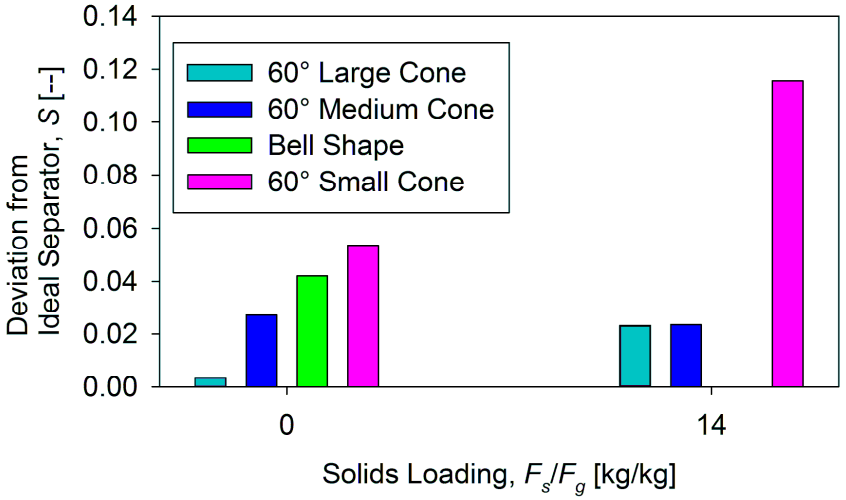

Figure 7 – Effect of Solids Loading on Gas Backmixing for All Tested Separator Designs (U_g = 0.80 m/s)

Gas-Solids Separation Efficiency Considerations

Huard (3) demonstrated that, in the same equipment used in this work, separator geometries that best preserved the solids' downward velocity and directed particles to the wall to form clusters were most efficient at removing solids from the exiting gas stream. Based on these results, the highest solids collection efficiency among the cone-shaped designs was expected for the largest cone diameter, which also demonstrated the least extensive gas backmixing among the tested separator designs. Using the same method to measure the solids collection efficiency as described in (3), the efficiency of all cone separator shapes was measured over several runs with varying solids loading but with identical gas velocity. The effect of solids loading was assumed to be negligible compared to the difference in efficiency between cone sizes. Fig. 8 compares the average solids collection efficiency and pulse response residual relative to the ideal case for each separator design. As expected, the highest collection efficiency was observed in the largest cone, and the efficiency decreased with decreasing cone size. The results in Fig. 8 confirm that the largest cone size had the highest collection efficiency and least extensive backmixing.

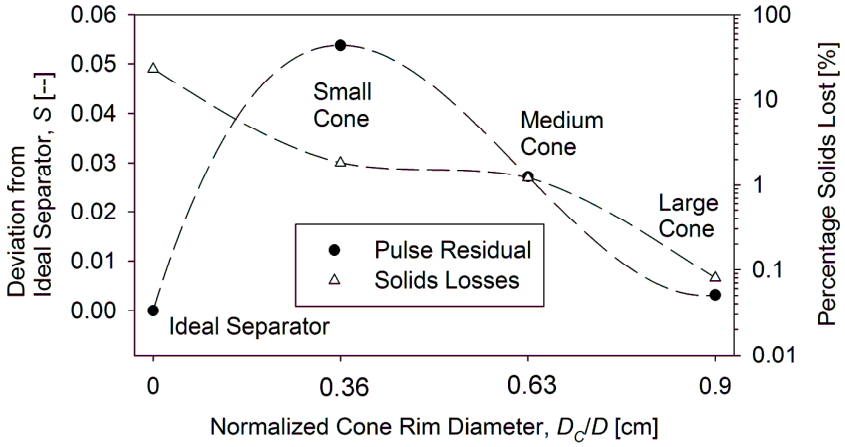

Figure 8 – Comparison of Gas Backmixing and Solids Losses for All Cone Separator Designs (U_g = 0.80 m/s)

CONCLUSION

A simple and effective pressure measurement technique was developed to rank several gas-solids separator designs according to the extent of backmixing that they induced in the gas phase of a gas-solids separator in a CFB downer reactor. Several separator designs were screened by measuring the separator's response in the pressure drop to a helium downstep. Using this method, a baseline case of minimal backmixing in the separation zone was established. All separator designs demonstrated greater backmixing than the baseline case. The largest, 6.3 cm diameter, 60° cone separator was selected as the best design, with 99.9% solids collection efficiency and acceptable backmixing at all solids loadings. The pressure measurement technique was also useful in identifying gas recirculation around the solids outlet. To minimize this harmful effect, a flow straightening honeycomb was placed at the solids outlet. This result also suggested future use of solids stripping gas below the gas outlet.

REFERENCES

1. A.T. Harris, J.F. Davidson, R.B. Thorpe. The influence of the riser exit on the particle residence time distribution in a circulating fluidised bed riser. Chem. Eng. Sci., vol. 58, pp. 3669-3680, 2003.
2. M. Huard, F. Berruti, C. Briens. Fast pyrolysis process intensification: study of the gas phase residence time distribution and backmixing in a downer reactor. Proc. Int. Conf. Circulating Fluidized Beds and Fluidization Technology, Sunriver, Oregon: 433-440, 2011.
3. M. Huard. An investigation of a novel gas-solid separator for downer reactors. M.E.Sc. Thesis. The University of Western Ontario, London, Ontario, Canada, 2009.
4. H. Brust, K.-E. Wirth. Residence time behavior of gas in a downer reactor. Ind. Eng. Chem. Res., 43: 5796-5801, 2004.
5. O. Levenspiel. Chemical Reaction Engineering. New York, NY: Wiley, 1999.
6. Y. Roques, T. Gauthier, R. Pontier, C. Briens, M.A. Bergougnou. Residence time distributions of solids in a gas-solids downflow transported reactor. Proceedings of Fourth International Conference on Circulating Fluidized Beds, Aug. 1-5, Hidden Valley, Pa., USA: 555-559 (1993).